Hindawi Publishing Corporation
International Journal of Corrosion
Volume 2014, Article ID 175094, 11 pages
http://dx.doi.org/10.1155/2014/175094

Research Article

Laboratory Assessment of Select Methods of Corrosion Control and Repair in Reinforced Concrete Bridges

Matthew D. Pritzl,[1] Habib Tabatabai,[2] and Al Ghorbanpoor[2]

[1] *Donan Engineering Co., Inc., 11321 Plantside Drive, Louisville, KY 40299, USA*
[2] *University of Wisconsin-Milwaukee, Department of Civil Engineering & Mechanics, 3200 North Cramer Street, Milwaukee, WI 53211, USA*

Correspondence should be addressed to Habib Tabatabai; ht@uwm.edu

Received 7 October 2013; Revised 23 January 2014; Accepted 7 February 2014; Published 10 April 2014

Academic Editor: W. Ke

Fourteen reinforced concrete laboratory test specimens were used to evaluate a number of corrosion control (CoC) procedures to prolong the life of patch repairs in corrosion-damaged reinforced concrete. These specimens included layered mixed-in chlorides to represent chloride contamination due to deicing salts. All specimens were exposed to accelerated corrosion testing for three months, subjected to patch repairs with various treatments, and further subjected to additional three months of exposure to accelerated corrosion. The use of thermal sprayed zinc, galvanic embedded anodes, epoxy/polyurethane coating, acrylic coating, and an epoxy patch repair material was evaluated individually or in combination. The specimens were assessed with respect to corrosion currents (estimated mass loss), chloride ingress, surface rust staining, and corrosion of the reinforcing steel observed after dissection. Results indicated that when used in patch repair applications, the embedded galvanic anode with top surface coating, galvanic thermal sprayed zinc, and galvanic thermal sprayed zinc with surface coating were more effective in controlling corrosion than the other treatments tested.

1. Introduction

Penetration of chlorides from deicing salts used on bridges causes significant long-term deterioration, which requires periodic maintenance and repair [1–3]. Corrosion of the reinforcing steel in concrete can lead to cracking and spalling concrete. Patch repairs are commonly used to address this problem. However, even when proper repair procedures are followed, failure of patches occurs in as little as 2–5 years [4].

The objective of this study was to assess relative performance of a number of corrosion control (CoC) procedures on patched chloride-contaminated reinforced concrete specimens tested under accelerated corrosion exposure in the laboratory. Fourteen specimens were exposed to accelerated corrosion testing for three months, subjected to patch repairs with various corrosion control treatments, and further subjected to an additional three months of exposure. The use of thermal sprayed zinc, galvanic embedded anodes, epoxy/polyurethane coating, acrylic coating, and an epoxy patch repair material was evaluated individually or in combination. The specimens were assessed with respect to corrosion currents (estimated mass loss), chloride ingress, surface rust staining, and corrosion of the reinforcing steel observed after dissection.

The phenomenon typically associated with patch failures, known as patch accelerated corrosion, occurs when the once "sound" area that surrounds the initial patch repair requires repair itself [4]. When traditional "chip and patch" repair procedures are used, a sudden change is introduced in the concrete surrounding the reinforcing steel as the bar crosses from old to new concrete (Figures 1 and 2). This occurs when new concrete (patch material), which is typically chloride-free and has a high pH, is placed adjacent to existing concrete, which is chloride-contaminated and has a lower pH. The interface creates zones of significantly different corrosion potentials along the steel bar. According to Ball

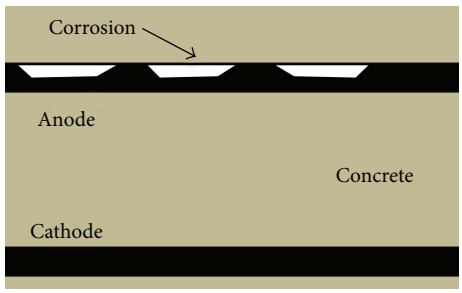

Figure 1: Corrosion cell in concrete.

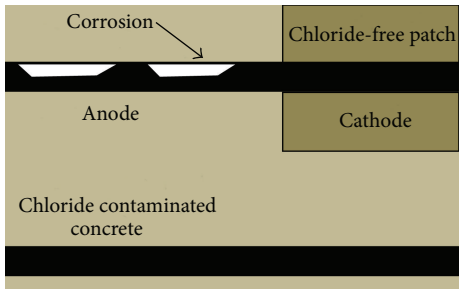

Figure 2: Patch-accelerated corrosion in concrete.

and Whitmore, this difference in corrosion potential causes formation of new corrosion sites in the surrounding chloride-contaminated concrete [4].

The patch-accelerated corrosion process (also referred to as the "ring anode" or "halo effect") occurs as the new concrete acts as an accelerant for corrosion. The steel bar within the new concrete can act as a cathode while the bar in the existing concrete acts as an anode. Evidence of this can be seen when spalls appear next to previously completed patch repairs [4].

In order to control further corrosion induced deterioration, strategies such as the use of concrete coatings, sealers, surfaced applied corrosion inhibitors, and cathodic protection have been used. Although coatings and sealers may work well for corrosion prevention, Tabatabai et al. found that surface applied treatments offered limited effectiveness when applied after the onset of corrosion [5].

Surface applied corrosion inhibitors, though not tested in this study, are applied on the hardened concrete surface and are intended to migrate through the pores of the concrete to protect the reinforcing bars from the ingress of harmful chemicals. El-Hacha et al. investigated the use of several surface applied corrosion inhibitors and concluded that the products tested "…generally helped delay and slow the corrosion process at the beginning, but none appeared to have totally stopped the corrosion process." El-Hacha et al. also concluded that "corrosion inhibitors seemed more effective at lower levels of chloride contamination and up to a threshold of about 0.5% by weight of cement" [6].

Cathodic protection (CP) makes use of an externally applied potential to shift all of the reinforcing steel into a cathodic and protected state. A 2001 Federal Highway Administration (FHWA) report concluded that "CP is only

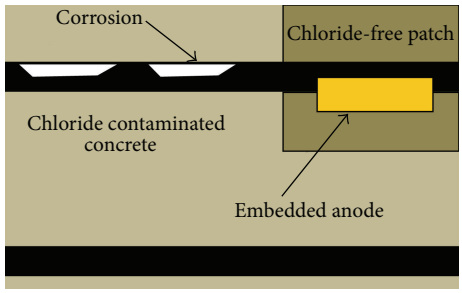

Figure 3: Intended action of discrete anode GCP in mitigating patch-accelerated corrosion.

rehabilitation technique that has been proven to stop corrosion is salt-contaminated bridge decks regardless of the chloride content of the concrete" [7].

Cathodic protection systems are divided into two categories: impressed current cathodic protection (ICCP) and galvanic cathodic protection (GCP). Discrete anode GCP systems (which are embedded within concrete) are intended to provide local protection and have been used in patch repairs to avoid the "ring anode" or "halo" effect. These discrete sacrificial anodes are attached to the reinforcing bars within the patch area. When attached to the newly cleaned steel within the patched area, the sacrificial anode, being more electronegative, will corrode in preference to the steel in the adjacent, nonpatched area (Figure 3). Because of this, the "ring anode" or "halo" effect is supposed to be mitigated [4].

A 2005 report by McMahan evaluated embedded galvanic units that were installed in the field in Vermont and were monitored for approximately 2 years. The report concluded that there were "…wide differences in monitored current, and presumably in corrosion rates and the amount of protection provided" and that the devices will "…only provide significant protection to concrete for 5 to 7 years" [8]. A 2007 paper by Dugarte et al. evaluated two types of commercial galvanic discrete anodes for reinforced concrete in both the field and laboratory. Based on preliminary findings, they concluded that "…only modest performance may be achieved with typical expected anode placement spacing in commonly encountered applications" [9].

Metalizing or thermal spraying is a method where a metal is melted and sprayed onto a prepared concrete surface. An electrical connection is then made between the embedded reinforcing steel and the sprayed metal. For reinforced concrete structures, the most commonly used thermal sprayed anodes are pure zinc and an aluminum-zinc-indium alloy (Al-Zn-In).

Daily and Green reported that the Al-Zn-In alloy will deliver more current than pure zinc in high resistivity environment (i.e., dry environments) because the indium keeps the anode more active [10]. However, Holcomb et al. suggested that a humectant can be added to pure zinc to increase moisture content at the zinc-concrete interface, thereby reducing the resistivity and increasing current output [11].

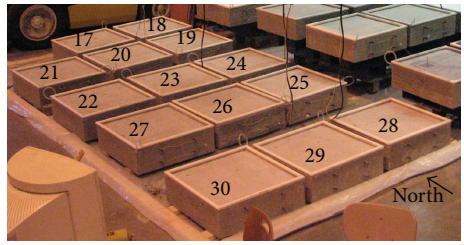

Figure 4: Experimental laboratory setup.

Table 1: Level of chlorides mixed into the CoC specimens (1 inch = 25.4 mm and 1.0 lb/yd^3 = 0.59 kg/m^3).

Depth (inch)	Average depth (inch)	% chlorides by mass of concrete	Chloride content by volume of concrete
0-1	0.5″	0.113%	4.41 lb/yd^3
1-2	1.5″	0.048%	1.87 lb/yd^3
2-3	2.5″	0.014%	0.55 lb/yd^3

In 2003, Whitney et al. studied the use of cathodic protection on substructure elements in the splash zone for the Queen Isabella Causeway in Texas. The report stated that the galvanic sprayed zinc and aluminum-zinc alloy systems "...both performed reasonably well." The report also noted that although the zinc was less expensive, the aluminum-zinc alloy appeared to perform more effectively in dryer conditions and provided more uniform protection [12].

An accelerated corrosion testing approach involving concurrent use of the impressed current technique and salt water exposure has been successfully implemented by a number of researchers. Examples include works by Ray et al. [13], Mullard and Stewart [14], Michel et al. [15], and Abaosara et al. [16].

El Maaddawy and Soudki studied accelerated corrosion testing of reinforcing steel in concrete by varying impressed current densities. The authors noted that, "up to 7.27% mass loss, accelerated corrosion using the impressed current technique was effective in inducing corrosion of the steel reinforcement in concrete" [17]. Austin et al. also studied the electrochemical behavior of steel-reinforced concrete during accelerated corrosion testing and concluded that "the impressed current technique has been confirmed to be an effective and quick method of accelerating chloride-induced corrosion" [18].

2. Materials and Methods

In this research, two (2) types of embedded discrete galvanic anodes, a humectant activated galvanic thermal sprayed zinc, a humectant activated galvanic thermal sprayed zinc with an epoxy/polyurethane coating, an embedded anode with an acrylic coating, a conventional cementitious patch repair material, and an epoxy patch repair material were chosen for evaluation. The thermal sprayed zinc and the various coatings were applied on the top surface of the concrete specimens. The epoxy/polyurethane coating involved a first coat of epoxy followed by a second coat of polyurethane.

2.1. Specimens and Materials. Fourteen reinforced concrete test specimens were cast (Figure 4). Ready-mixed air-entrained concrete, containing fly ash, was used to fabricate the test specimens. The concrete was specified to meet the governing specifications for bridge deck construction in Wisconsin with a specified minimum 28th day compressive strength of 4,000 psi (27.6 MPa). The reinforced concrete test specimens had dimensions of 28 in. (71.1 cm) × 28 in. (71.1 cm) × 8 in. (20.3 cm). Number 5 reinforcing bars (diameter of 5/8 in. or 15.9 mm) meeting the requirements of ASTM A615 M were used as shown in Figure 5. Curing consisted of covering the specimens with plastic sheathing for seven days. The average measured 28-day compressive strength of three concrete cylinders was 5,839 psi (40.3 MPa).

These 14 specimens (numbered 17 through 30) were part of a total of 30 such specimens that included 16 additional specimens for a companion study. To reduce the length of time needed for chlorides to reach the top steel layer, the top layer of reinforcement utilized a 1 in. (2.5 cm) clear cover. A standard 2 in. (5.1 cm) clear cover was used for the bottom layer of reinforcement. PVC pipe was caulked to the perimeter of the top surface of the concrete specimens to create the reservoir that periodically held the salt laden water (Figures 4 and 5). To better replicate chloride contaminated concrete, these 14 specimens were cast with layers of premixed chlorides. The bottom 5 in. (12.7 cm) of the specimens was cast without added chlorides while the upper 3 in. (7.6 cm) was cast with chloride profiles representative of common bridge deck conditions in the northern deicing states at a bridge age of 10 years.

Using chloride diffusion coefficient (D) and surface chloride concentration (C_0) from a Strategic Highway Research Program (SHRP) paper by Weyers et al. [19] and Fick's 2nd law of diffusion, a chloride profile that represented 10 years of exposure to chlorides was utilized. Based on the results of the SHRP study, a "D" of 0.11 in^2/yr (0.71 cm^2/yr) and a "C_0" of 5.985 lb/yd^3 (3.55 kg/m^3, representative of the mean of all the collected data) were used to determine the level of chlorides to be added in each of the three top layers of concrete.

Table 1 presents the chloride levels that were added to the specimens. The percentage values shown are based on a concrete unit weight of 145.0 lb/ft^3 (2,345 kg/m^3).

At an average depth of 1.5 in. (3.8 cm), which is at the level of reinforcing steel in this project, the chloride content was nearly two times the corrosion threshold of 1.0 to 1.5 lb/yd^3 (0.59 kg/m^3 to 0.89 kg/m^3) indicated by ACI 222 [20].

During the concrete pour, the bottom 5 inches (12.7 cm) of the CoC specimens was first placed. The three chloride profile levels were then added in succession. Concrete was mixed with table salt in a concrete mixer. When the pour was completed, all of the specimens were covered with a sheet of plastic for seven days.

The specimens were subjected to three months of exposure to accelerated corrosion (described later). After 3 months of exposure, the specimens were examined and tested for

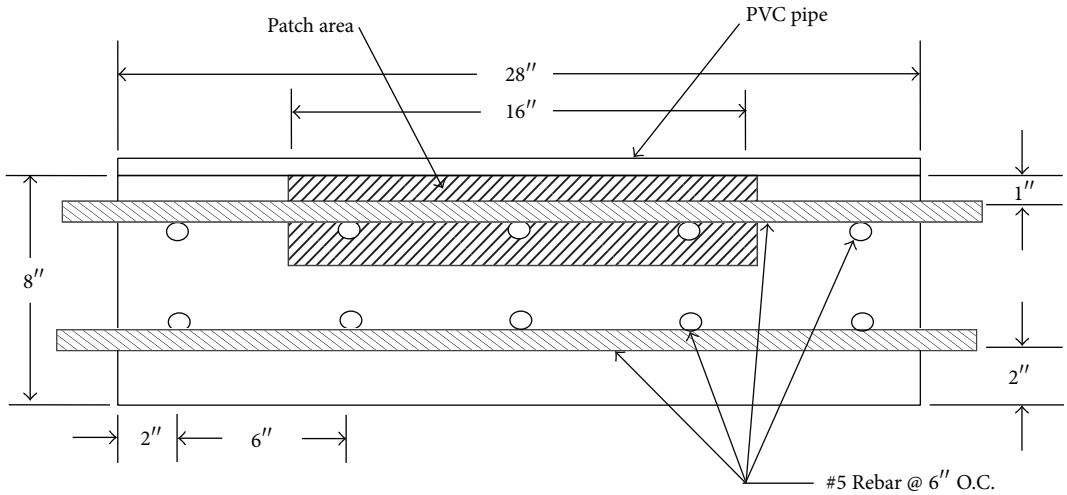

Figure 5: Cross-section of concrete specimens.

Table 2: Table of treatments used for each specimen*.

Specimen number	Type of treatments	General description	Referred to as
17 and 18	Control	No treatment	Control
19 and 20	Thermal sprayed galvanic anode with coating applied on top surface of specimen	Humectant activated thermal sprayed zinc with epoxy/polyurethane coating	TSZ w/EP-C
21 and 22	Thermal sprayed galvanic anode applied on top surface of specimen	Humectant activated thermal sprayed zinc	TSZ
23 and 24	Embedded galvanic anode placed within patch area	Cylindrical-shaped zinc anode	EA-A
25 and 26	Embedded galvanic anode placed within patch area with acrylic coating applied on top surface of specimen	Cylindrical-shaped zinc anode with acrylic coating	EA-A w/A-C
27 and 28	Embedded galvanic anode placed within patch area	Box-shaped zinc anode	EA-B
29 and 30	Epoxy repair mortar as a patch material	Epoxy resins and polyamino amine adducts	EM

*Specimens 17 through 28 included a conventional cement-based patch material in addition to the treatments shown. Specimens 29 and 30 included an epoxy patch material. All patching and treatments were applied after 3 months of exposure to accelerated corrosion.

chloride ingress. Patch repairs were then performed (Figure 6) and the various treatments were applied. The patch repair consisted of saw-cutting the perimeter of the square patch area (16 in. (40.6 cm) × 16 in. (40.6 cm)), chipping out the concrete, cleaning the exposed reinforcing steel bar with a drill and wire wheel accessory, applying an epoxy coating to the steel bar, applying a bonding agent to the concrete substrate, and placing the patch repair material. The coating of the steel bar and the application of bonding agent within the patch area were based on patch material manufacturer's instructions and in accordance with conventional patch repair practices. Following anode installation directions, care was taken not to coat the points of electrical continuity (locations where the bars intersect), the connections of the anodes to the reinforcing steel, or the anodes themselves.

Table 2 describes the treatment(s) used on each specimen. The numbers on the specimens in Figure 4 correspond to the specimen numbers in Table 2. While the embedded anodes were attached directly to the exposed bars, the thermal sprayed zinc and surface coatings were applied on the top surface of the concrete specimen and patched areas.

Two types of patch materials were used: a conventional material and a proprietary epoxy-based material. The conventional patch repair material used on specimens 17 through 28 was a commercial cement-based, rapid strength gain, patching and repair mortar which contained a migratory corrosion inhibitor. According to the manufacturer, the patch material is compatible with galvanic anodes. The epoxy patch repair material utilized on specimens 29 and 30 is reported by the manufacturer to be a three component, solvent-free, high performance epoxy mortar.

Epoxy bonding agents for coating of substrate concrete (within the patch area) were recommended by the manufacturer of the conventional patches. Yet, epoxy bonding agents are generally not recommended for use with galvanic anodes.

Table 3: Steel loss of CoC specimens after 3-month exposure and 6-month exposure.

Specimen number	Treatment	0–3-month steel loss (g)	3–6-month steel loss (g)	3–6-month index	0–6-month steel loss (g)	0–6-month index
17 and 18	Control	357.2	148.7	1.3	505.9	2.8
19 and 20	TSZ w/EP-C	336.4	73.6	0.1	410.0	1.2
21 and 22	TSZ	313.3	90.6	0.4	403.9	1.1
23 and 24	EA-A	338.1	175.8	1.8	513.9	2.9
25 and 26	EA-A w/A-C	278.2	78.3	0.2	356.5	0.3
27 and 28	EA-B	295.4	169.2	1.7	464.6	2.1
29 and 30	EM	289.0	275.4	3.4	564.4	3.8

Table 4: Comparison of initial intended and average acid-soluble chloride contents of CoC specimens (% chlorides by concrete weight) at 0 month (1 inch = 25.4 mm).

Depth	Initial intended plus baseline chlorides	Average of initial measured chlorides	Average initial measured chlorides
$0''$ to $\frac{1}{4}''$	0.155	0.183	0.156
$\frac{1}{4}''$ to $\frac{1}{2}''$		0.171	
$\frac{1}{2}''$ to $\frac{3}{4}''$		0.142	
$\frac{3}{4}''$ to $1''$		0.129	
$1''$ to $1\frac{1}{4}''$	0.090	0.119	0.106
$1\frac{1}{4}''$ to $1\frac{1}{2}''$		0.109	
$1\frac{1}{2}''$ to $2''$		0.089	
$2''$ to $2\frac{1}{2}''$	0.056	0.073	0.065
$2\frac{1}{2}''$ to $3''$		0.057	

Table 5: Comparison of average acid-soluble chloride contents of CoC specimens at 0 month and after 3 months (1 inch = 25.4 mm).

Depth	Average of 0-month chlorides	Average of 0-month chlorides per inch	Average of 3-month chlorides	Average of 3-month chlorides per inch
$0''$ to $\frac{1}{4}''$	0.183	0.156	0.502	0.322
$\frac{1}{4}''$ to $\frac{1}{2}''$	0.171		0.367	
$\frac{1}{2}''$ to $\frac{3}{4}''$	0.142		0.243	
$\frac{3}{4}''$ to $1''$	0.129		0.174	
$1''$ to $1\frac{1}{4}''$	0.119	0.106	0.131	0.108
$1\frac{1}{4}''$ to $1\frac{1}{2}''$	0.109		0.113	
$1\frac{1}{2}''$ to $2''$	0.089		0.099	
$2''$ to $2\frac{1}{2}''$			0.088	

However, epoxy bonding agents can be used with embedded anodes if both the metallic and ionic paths are maintained. Since the metallic path had already been confirmed (through the connection between the anode and the bars), the ionic path from the anode to the cathode had to be provided as well. For the discrete anodes, this was accomplished by not coating the anodes or the substrate concrete immediately below the anodes. When using epoxy bonding agents in specimens that received thermal sprayed metals, the ionic path will still reach the bars in the areas inside and outside of the patch with direct contact to the top surface of each specimen.

The manufacturer of the conventional patch material recommended the use of an epoxy bonding agent and the manufacturer of the epoxy patch repair material specified a concrete primer on the surface of the concrete substrate within the patch area. We chose to use an epoxy bonding agent in conjunction with the conventional patch repair materials in accordance with manufacturer's recommendation, following all guidelines applicable for concurrent use of embedded anodes. Moreover, all guidelines for the epoxy patch repair material were followed.

2.2. Experimental Methods. The treatments in question were evaluated with respect to corrosion currents, chloride ingress, extent of cracking, severity of rust staining, and visual inspection of the reinforcing steel after the conclusion of testing and dissection.

To accelerate the corrosion process, the specimens were subjected to wetting/drying cycles and a reverse cathodic protection system. Cycles of one week wet (using a 6% NaCl solution on the top surface) and one week dry (no saltwater ponding) were utilized. A reverse cathodic protection system was created by continuously applying a regulated voltage of 9 V from the positive terminal of the regulated power supply to the top layer of reinforcement (the anode). A 1 Ω precision resistor located between the positive terminal and the anode

Figure 6: Patch repairs of laboratory specimens.

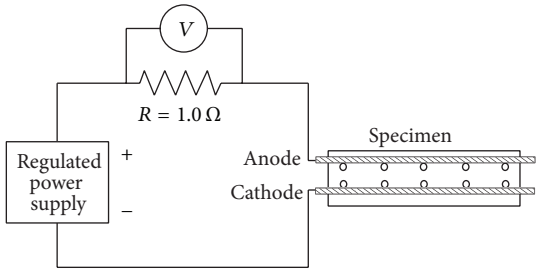

Figure 7: Corrosion cell for laboratory specimens.

was used to facilitate measurement of current (Figure 7). The voltage across the 1 Ω resistor was manually recorded each day on all specimens using a high impedance multimeter.

The measured corrosion currents were used to estimate the amount of steel loss that had occurred for comparison purposes. The amount of steel loss was estimated using Faraday's Law (1),

$$m = \frac{A^{\text{tm}}C}{Fz}, \tag{1}$$

where m = loss of mass, A^{tm} = atomic mass of the reaction ion (55.85 g/mol for iron), C = total charge that has passed through the circuit = $\int I(t)dt$, $I(t)$ = measured corrosion current at time (t), F = Faraday's constant (96485 C/mol), and Z = valence of reaction (assumed to be 2).

The chloride content of all specimens was determined by analyzing drilled concrete samples at various depths using the Rapid Chloride Test (RCT) method [21]. Acid soluble chloride levels were measured as a percentage of concrete mass. Regression analyses utilizing Fick's 2nd Law (2) and Microsoft Excel's solver function were utilized to further analyze the chloride content results and to provide a direct comparison among the specimens,

$$C_{(x,t)} = C_0\left(1 - \text{erf}\,\frac{x}{2\sqrt{Dt}}\right), \tag{2}$$

$C_{(x,t)}$ = chloride concentration at depth x and time t, C_0 = surface chloride diffusion (lb/yd^3 or kg/m^3), erf = error function (a mathematical function), and D = chloride diffusion coefficient (in^2/yr or cm^2/yr).

Prior to patch repairs, the extent of rust staining seen on the concrete surface was evaluated visually and quantified. The exposed reinforcing steel was visually evaluated for extent of corrosion after the concrete in the patch area was removed.

Periodically, half-cell potential readings were taken. The readings were taken at sixteen locations per specimen. Furthermore, detailed crack maps were generated at 0-month, 3-month, and 6-month exposure. The widths of the cracks were measured using a standard crack width comparator. At the conclusion of testing, the extent of rust staining on the concrete surface was evaluated visually. Finally, the specimens were dissected and the embedded reinforcing steel was visually assessed for extent of corrosion.

The results of the various measurements (as discussed in Section 3) were given numerical indices (3) according to a scale of 0 (minimum) to 4 (maximum). The actual value is the value associated with the parameter of interest for each specimen, while the minimum and maximum values used in (3) are based on the minimum and maximum values observed across all specimens. For example, the minimum and maximum steel loss values across all specimens corresponded to ratings of 0 and 4, respectively,

$$\text{Index} = \left(\frac{(\text{actual value}) - (\text{minimum value})}{(\text{maximum value}) - (\text{minimum value})}\right) \times 4. \tag{3}$$

3. Results and Discussion

A detailed report of this experimental program and its individual results is provided by Tabatabai et al. [22]. In the following discussion, the average results are shown for brevity. Individual results for companion specimens used in averaging were in reasonable agreement.

3.1. Corrosion Currents. A plot of average corrosion current versus time for the specimens is shown in Figure 8. As expected, the corrosion currents increased during the wet periods (shaded region) and decreased during the dry periods.

From the initiation of testing until 3 months (90 days), there appears to be reasonable agreement among all specimens (as expected). The break in the graph between 3 months (90 days) and the continuation of the project at 270 days was due to the time necessary to perform the chloride testing and patch repairs. Accelerated testing (including the 9 V electrical potential) was restored after 270 days and continued for another three months.

After patch repairs, the TSZ, EA-A w/A-C, and TSZ w/EP-C treatments all displayed a decrease in corrosion current, while the currents associated with the Control and EM specimens increased initially and then decreased. It is believed that the rapid increase in corrosion current for the EM was due to the widely dissimilar properties of the epoxy patch repair material compared with the surrounding concrete. A reinforcing bar crossing from the substrate concrete into the new epoxy material would likely develop more pronounced anode and cathode area on the bar. Meanwhile, EA-A and EA-B also exhibited an increase in corrosion current over time after treatment.

Table 6: Calculated chloride diffusion coefficients for patch materials of CoC specimens at the conclusion of project (1 inch = 25.4 mm).

Specimen number	Patch treatment		C_0 (% Cl by concrete mass)	$D_{\text{Treatment}}$ (in^2/yr)	Index
17 and 18	Control	(Conventional repair material)	0.445	0.030	2.8
19 and 20	TSZ w/EP-C			0.010	0.9
21 and 22	TSZ			0.004	0.4
23 and 24	EA-A			0.010	0.9
25 and 26	EA-A w/A-C			0.005	0.4
27 and 28	EA-B			0.021	1.9
29 and 30	EM			—	—

Table 7: Rating of concrete staining and reinforcing steel for CoC specimens after 6 months.

Specimen number	Individual Rebar								"in" Rebar average	Surface staining	Total rating
	A	B		C		D		E			
	out	in	out	in	out	in	out	out			
17 and 18	4.0	3.0	4.0	3.0	3.5	3.0	4.0	4.0	3.0	0.5	3.5
19 and 20	3.0	3.5	4.0	3.0	3.5	4.0	4.0	4.0	3.5	0.0	3.5
21 and 22	4.0	3.5	4.0	3.0	4.0	4.0	4.0	3.5	3.5	0.0	3.5
23 and 24	4.0	4.0	4.0	2.5	3.0	4.0	4.0	4.0	3.5	1.0	4.5
25 and 26	3.5	4.0	4.0	3.0	4.0	4.0	4.0	3.0	3.7	0.0	3.7
27 and 28	3.0	3.5	4.0	2.5	3.5	4.0	4.0	4.0	3.3	2.0	5.3
29 and 30	3.5	3.0	4.0	3.0	4.0	3.5	4.0	4.0	3.2	3.0	6.2

Table 8: Half-cell potential readings after 3 months.

Specimen number	Future treatment	Average (mV)	Std Dev. (mV)
17 and 18	Control	−541.1	27.9
19 and 20	TSZ w/EP-C	−540.6	27.3
21 and 22	TSZ	−532.7	28.1
23 and 24	EA-A	−542.9	22.7
25 and 26	EA-A w/ A-C	−554.2	24.9
27 and 28	EA-B	−556.8	32.3
29 and 30	EM	−554.3	18.2

3.2. Steel Loss. By utilizing the aforementioned corrosion currents and (1), the amount of steel loss was estimated (Table 3). Numerical integration was used to calculate the total charge used in estimating steel loss.

For the 0–3 month data, the average steel loss was calculated to be 315.4 g (0.70 lb) with a standard deviation of 35.4 g (0.08 lb). Based on the initial steel loss values, it appears that all specimens were in a reasonably similar condition after the first 3 months of laboratory testing.

For the 3–6 month steel loss data, the TSZ w/EP-C, EA-A w/A-C, and TSZ produced the lowest indices. When considering the 0–6 month index, EA-A w/A-C, TSZ, and TSZ w/EP-C had the lowest Index values. Therefore, it can be concluded that these three treatments performed better with regard to theoretical steel loss due to corrosion. It is interesting to note that all these better-performing treatments incorporated some form of coating or physical barrier on the top surface of the specimen.

3.3. Chloride Ingress. The baseline chloride content was taken from virgin concrete. The average measured chloride content of the virgin concrete was found to be 0.042% by concrete weight or approximately 1.65 lb/yd^3 (0.98 kg/m^3) of concrete. This measured chloride content was relatively high. An earlier study by Tabatabai et al. has similar results and found that the source of the chlorides was from coarse limestone aggregates [5].

Prior to exposure to accelerated corrosion, the chloride contents of all 14 specimens were evaluated at average depths of 1/4 in. (0.64 cm), 1/2 in. (1.27 cm), 3/4 in. (1.91 cm), 1 in. (2.54 cm), 1.25 in. (3.18 cm), 1.5 in. (3.81 cm), 2 in. (5.08 cm), 2.5 in. (6.35 cm), and 3 in. (7.62 cm), so that confirmation of the actual mixed-in chloride contents could be made. Three locations, for a total of 27 chloride tests per specimen, were analyzed. Chloride testing (Table 4) revealed that the actual chloride contents were in reasonable agreement with the "initial intended plus baseline chloride" profile.

By utilizing regression analyses of measured chlorides, the agreement between the "initial intended" and "initial measured" chlorides could be further verified. Using a time of 10 years (assumed for calculating the amount of mixed-in chlorides), C_0 was found to equal 0.149% chlorides by concrete weight (5.83 lb/yd^3 or 3.46 kg/m^3) and D_{avg} was found to equal 0.150 in^2/yr (0.97 cm^2/yr), with a standard deviation of 0.026 in^2/yr (0.17 cm^2/yr). These values are in reasonable agreement with the values of C_0 = 0.153% (6.0 lb/yd^3 or

Table 9: Condition summary of CoC specimens after 6 months of exposure.

Specimen number	Treatment	6-month CoC ratings			Total (out of 16)
		Steel loss (out of 4)	Patch chloride content (out of 4)	Rebar corrosion and staining (out of 8)	
17 and 18	Control	2.80	2.80	3.50	9.10
19 and 20	TSZ w/EP-C	1.25	0.90	3.50	5.65
21 and 22	TSZ	1.10	0.35	3.50	4.95
23 and 24	EA-A	2.90	0.90	4.50	8.30
25 and 26	EA-A w/A-C	0.35	0.40	3.67	4.42
27 and 28	EA-B	2.10	1.95	5.33	9.38
29 and 30	EM	3.75	—*	6.17	—*

*Patch chloride content did not conform to Fick's 2nd Law.

3.56 kg/m^3) and D = 0.110 in^2/yr (0.71 cm^2/yr) that were used initially to determine the mixed-in chloride levels.

Prior to removing concrete from the specimens for patch repair, the specimens were again evaluated for chlorides after 3 months of accelerated corrosion testing. Testing was performed at 1/4 in. (0.64 cm) intervals to a depth of 2 in. (5.08 cm) at 3 locations per specimen. Table 5 compares the average measured chloride contents at 0 and 3 months.

From Table 5, it is clear that the chlorides were effectively drawn into top 1 in. (2.54 cm) of the concrete during the first 3 months of exposure. The average chloride content in the top 1-inch (2.54 cm) of concrete more than doubled in the 3-months of accelerated corrosion testing.

An optimization analysis using the "3-month measured chlorides," minus the base-line chlorides, with a time of 0.25 years (3 months), revealed that the following parameters of Fick's 2nd Law best fit the experimental data: C_0 = 0.514% by concrete weight (20.12 lb/yd^3 or 11.9 kg/m^3) and D_{avg} = 1.375 in^2/yr (8.87 cm^2/yr) with a standard deviation of 0.565 in^2/yr (3.65 cm^2/yr).

The agreement between the intended, measured, and calculated chlorides (based on regression) is shown in Figure 9 (for specimen number 17, a control specimen). This representative graph compares the measured concrete chlorides before the start of accelerated corrosion with the intended (by mixing salt) chloride profile plus the chloride level existing in the concrete itself (base-line chloride). This graph also compares the measured chlorides at 3 months with the projected chlorides at 3 months based on estimated D and C_0 values.

Prior to patch repairs, the average base-line chloride content of the conventional repair material was found to be 0.008% by concrete weight. This level of chlorides is well within the accepted limits. The base-line chloride content of the EM was found to be 0.001% chlorides by weight.

After exposure to additional three months of accelerated corrosion testing, the CoC specimens were again tested for chloride ingress. Chloride testing was performed at locations in the original (substrate) concrete as well as in the patch area.

For the substrate concrete, the chloride profiles of most specimens did not agree with Fick's Law. Therefore, the use of regression in analyzing the substrate concrete after 6 months of exposure was not warranted. However, the chloride contents of the substrate concrete were not used in evaluating the performance of the treatments within the patch repair materials. Chloride testing of the substrate concrete was performed to show that chlorides continued to penetrate the concrete. It should be noted that specimens number 19 through 22 (those with thermal sprayed zinc) had nonconforming chloride levels at a depth of 1/4 in. (0.64 cm) only. It is believed that the TSZ (zinc anode) attracts and retains negatively charged chloride ions near the surface, thus causing deviation from Fick's 2nd Law.

Analysis of the chloride testing data for the patch repair materials after additional 3 months of testing revealed that, in general, chlorides were only drawn into the top 1/4 in. (0.64 cm) of the patch repair materials. Table 6 shows the estimated C_0 and D values for the patch materials after 3 months of exposure based on an optimization analysis assuming that Fick's Law applies.

As displayed in Table 6, TSZ and EA-A w/A-C appeared to be the most effective in reducing the ingress of chlorides into the conventional patch repair materials. The specimens with epoxy mortar (EM) had low chloride contents; however, the distribution was not consistent with Fick's Law. Therefore, a "D" value is not reported for EM specimens.

3.4. Surface Staining and Steel Corrosion. To provide a quantitative measure of the condition of the specimens after exposure to accelerated corrosion testing, a visual examination of the rust staining on the concrete surface and exposed reinforcing steel was performed, so that a numerical rating could be assigned to each specimen. The condition of the CoC specimens after 6 months of exposure and dissection is shown in Figures 10 and 11, respectively.

Based on a rating scale of 0 to 4, with 0 being the best condition and 4 being the worst condition, rust staining on the surface of the specimens as well as the level of section loss in the reinforcing steel was evaluated. The rating scale for staining was based purely on visual examination; the more severe the staining, the higher the grade. The rating scale for the condition of the reinforcing steel was based on the loss

of ribs (Figures 12 and 13). If no corrosion by-products were present, a rating of 0 was given. If it appeared that all of the ribs were lost, a rating of 4 was given. If, on average, 1/4, 1/2, or 3/4 of the ribs were lost, ratings of 1, 2, and 3 were given, respectively. This rating was given to each of the top-layer bars in each specimen. The ratings were then averaged for each specimen. The two separate ratings (staining and loss of steel section) were then added together, for a maximum value of 8, to determine a combined rating.

After the initial 3 months of exposure, it was found that the average rating for the exposed reinforcing steel (within the excavated patch area) was 3.0 and that the average rating for the staining was 3.0. The average 3-month total (steel bar plus staining) rating for all CoC specimens was 6.0.

Table 7 presents the individual and final ratings for each of the specimens after 6 months of exposure. In Table 7, the five reinforcing bars (in the top layer in each specimen) are designated A through E. Rebar A is located at the west end of the specimens, Rebar B through Rebar D are located within the patch, and Rebar E is located on the east end of the specimens.

All exposed bars were rated; however, only the Rebar that was used within the patch repairs ("in" bars) was counted toward the bar rating (bars B through D). Bars outside of the patch area ("out" bars) were not counted toward the rating of the steel rebar. In doing so, a comparison could be made with the ratings that were made prior to patch repairs. Concrete surface staining was also similarly rated.

3.5. Half-Cell Potential. Half-cell measurements utilizing a copper-copper sulfate electrode were obtained for each of the concrete specimens. Prior to measurement, the accelerated corrosion system was turned off for a day and the slabs were saturated with tap-water. Readings were made after 3 months. It was found that the average potential was −546.1 mV with a standard deviation of −28.4 after three months of exposure (Table 8). Because the readings were fairly uniform, contour plots were not made. Since these readings were more negative than −350 mV, a 90% probability of corrosion was indicated after 3 months of exposure in the CoC specimens [2]. Half-cell potential testing was not performed after 6 months of exposure because of the high potential levels found at 3 months in all specimens and because of a number of coatings applied on the top surface of specimens that would prevent half-cell potential measurements.

3.6. Discussion. The following section provides a summary and discussion of the results of this study. Based on chloride content, reinforcing steel corrosion, concrete surface staining, and half-cell potential testing, the CoC specimens appeared to be in a similar condition after the first 3 months of accelerated corrosion testing. Therefore, it can be concluded that the addition of chlorides to the concrete mix, "ponding" of salt water, and application of electric current were controlled properly during the first 3 months of exposure and all specimens (similarly prepared and exposed for 3 months) were responding similarly.

A summary of numerical ratings for the CoC specimens after 6 months of exposure is presented in Table 9. For this evaluation, the chloride content of the substrate concrete was not used in evaluating the effectiveness of the treatments within the patch repair and only the "in" patch reinforcing steel, along with surface staining (including substrate concrete), was used for the rating.

Based on the results of Table 9, EA-A w/A-C, TSZ, and TSZ w/EP-C appeared to be the most effective in controlling corrosion. It is important to note that all these treatments incorporated some form of coating or physical barrier applied on the top surface of specimens; however, none of the CoC specimens had a coating treatment alone to conclusively assess whether the coating is the sole determining factor.

When evaluating the patched areas of the TSZ and TSZ w/EP-C specimens, it is interesting to note that the steel bar near the connection point to the thermal sprayed zinc exhibited more corrosion than other areas of the steel bar.

The patches containing the EA-A (without coating) and EA-B were no more effective in controlling corrosion than the control specimens. Chloride measurements indicated that the anodes attracted chlorides to their vicinity. These chloride "hot spots" increased corrosion of the reinforcing steel in the area of attachment to the anodes.

In regard to the EM specimens, the high initial corrosion currents and associated steel loss appear to be the result of the highly dissimilar material properties. A "ring-anode" effect became visible at the interface of the patch and substrate concrete over the duration of testing. Although the EM patch material itself did not display any signs of cracking, the existence of the "ring-anode" effect at the perimeter of the patch was clearly evident. These were the only specimens to significantly display this phenomenon.

It appeared that the conventional patch repair material performed well (i.e., patch itself did not deteriorate). This was evidenced by the fact that no significant cracking was present on any of the patched areas at the conclusion of testing. However, as stated earlier, the performance of the patch material is not an overall indication of performance of patch due to the "halo effect."

4. Conclusions

Based on the observation of the test specimens subjected to an accelerated corrosion regime, the following conclusions are made.

(1) Embedded anode A with acrylic coating (EA-A w/A-C), thermal sprayed zinc (TSZ), and thermal sprayed zinc with epoxy/polyurethane coating (TSZ w/EP-C) were most effective in controlling corrosion. It appears that the main factor for the better performance of these specimens was the presence of some form of coating or physical barrier.

(2) The performance of the embedded anodes (EA-A without coating as well as EA-B without coating) was not better than the control specimens.

(3) For the epoxy patch repair material (EM), the initial increase in corrosion current and appearance of

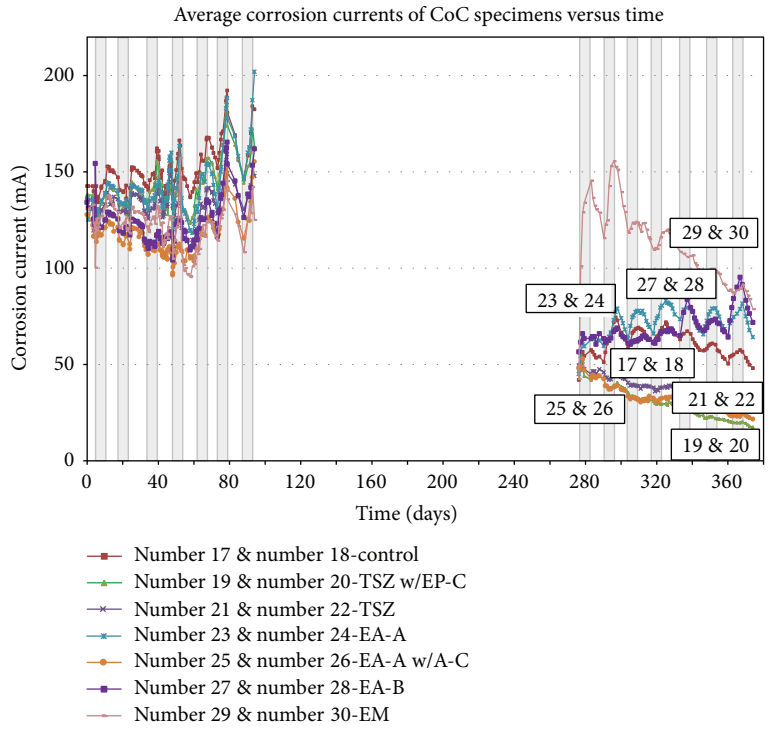

Figure 8: Average corrosion currents of specimens.

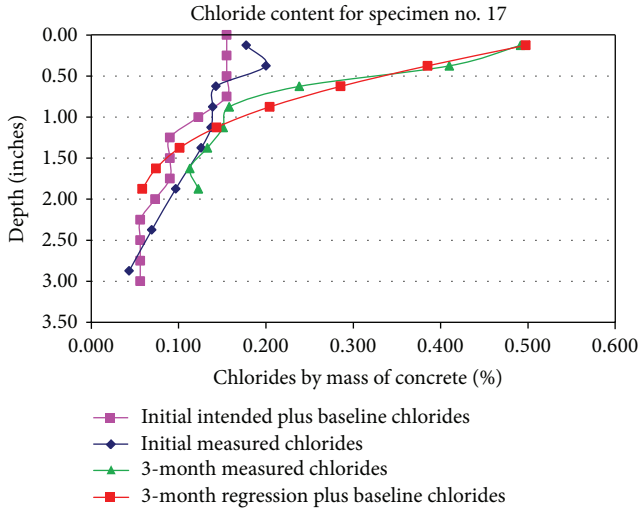

Figure 9: Comparison of initial and 3-month chlorides for specimen number 17.

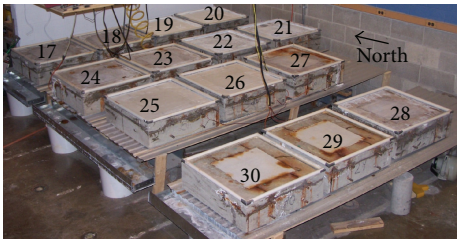

Figure 10: Surface staining on laboratory CoC specimens after 6 months.

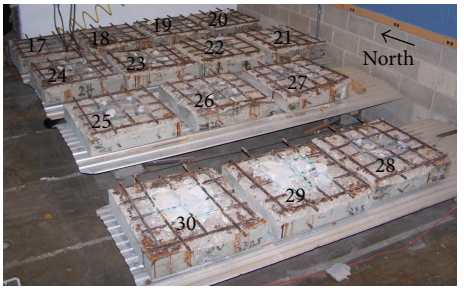

Figure 11: Dissected laboratory CoC specimens.

the "ring-anode" effect at the perimeter of the patch is due to the significant dissimilarity between epoxy mortar and concrete.

Conflict of Interests

The authors declare that there is no conflict of interests regarding the publication of this paper.

Acknowledgments

The authors wish to express their gratitude and sincere appreciation to the Wisconsin Highway Research Program for funding this effort. The project team would also like to thank Ambassador Steel of Waukesha, Wisconsin, for

Figure 12: Steel rating of 2 and 3 (close-up of exposed Rebar of control after 3 months).

Figure 13: Steel rating of 4 (close-up of exposed Rebar of TSZ w/EP-C after 6 months).

donating materials, Masonry Restoration, Inc. of Milwaukee, Wisconsin, for lending their demolition equipment, Aaron Coenen, John Condon, Chin Wei-Lee, Cory Schultz, and Rahim Reshadi for assisting with the placement of concrete, and Dr. Tracy Pritzl for her assistance with chloride testing.

References

[1] United States Department of Transportation Federal Highway Administration Turner-Fairbank Research Center, 1998, Corrosion Protection: Concrete Bridges, Turner-Fairbank Research Center, http://www.tfhrc.gov/structur/corros/corros.htm.

[2] P. H. Emmons, *Concrete Repair and Maintenance Illustrated*, RS Means, Kingston, Mass, USA, 1993.

[3] M. El-Reedy, *Steel-Reinforced Concrete Structures: Assessment and Repair of Corrosion*, Taylor & Francis Group, Boca Raton, Fla, USA, 2008.

[4] C. J. Ball and D. W. Whitmore, *Corrosion Mitigation Systems For Concrete Structures*, Concrete Repair Bulletin, 2003.

[5] H. Tabatabai, A. Ghorbanpoor, and A. Turnquist-Nass, *Rehabilitation Techniques For Concrete Bridges*, Wisconsin Department of Transportation Research and Library, Madison, Wis, USA, 2005.

[6] R. El-Hacha, A. Mirmiran, A. Cook, and S. Rizkalla, "Effectiveness of surface-applied corrosion inhibitors for concrete bridges," *Journal of Materials in Civil Engineering*, vol. 23, no. 3, pp. 271–280, 2011.

[7] United States Department of Transportation Federal Highway Administration Research and Development, 2001, Long-Term Effectiveness of Cathodic Protection Systems on Highway Structures, McLean.

[8] J. McMahan, *Preliminary Evaluation of Galvashield Installation in BR 48, I-89, Waterbury*, Vermont Agency of Transportation, Montpelier, Vermont, 2005.

[9] M. Dugarte, A. A. Sagüés, R. Powers, and I. Lasa, "Evaluation of point anodes for corrosion prevention in reinforced concrete," Tech. Rep. 07304, NACE International, Houston, Tex, USA, 2007.

[10] S. F. Daily and W. K. Green, "Galvanic cathodic protection of reinforced and prestressed concrete structures using CORRYSPRAY—a thermally sprayed aluminum alloy," Tech. Rep., Corrpro Companies.

[11] G. R. Holcomb, B. S. Covino Jr., S. D. Cramer et al., *Humectants To Augment Current From Metallized Zinc Cathodic Protection Systems on Concrete*, Oregon Department of Transportation, Salem, Mass, USA, 2002.

[12] D. Whitney, L. Elcheverry, and H. Wheat, *Cathodic Protection: Coordinating Corrosion To Save State Structures*, Center for Transporation Research: The University of Texas at Austin, Austin, Tex, USA, 2003.

[13] I. Ray, G. C. Parish, J. F. Davalos, and A. Chen, "Effect of concrete substrate repair methods for beams aged by accelerated corrosion and strengthened with CFRP," *Journal of Aerospace Engineering*, vol. 24, no. 2, pp. 227–239, 2011.

[14] J. A. Mullard and M. G. Stewart, "Corrosion-induced cover cracking: new test data and predictive models," *ACI Structural Journal*, vol. 108, no. 1, pp. 71–79, 2011.

[15] A. Michel, B. J. Pease, M. R. Geiker, H. Stang, and J. F. Olesen, "Monitoring reinforcement corrosion and corrosion-induced cracking using non-destructive x-ray attenuation measurements," *Cement and Concrete Research*, vol. 41, no. 11, pp. 1085–1094, 2011.

[16] L. Abosrra, A. F. Ashour, and M. Youseffi, "Corrosion of steel reinforcement in concrete of different compressive strengths," *Construction and Building Materials*, vol. 25, no. 10, pp. 3915–3925, 2011.

[17] T. A. El Maaddawy and K. A. Soudki, "Effectiveness of impressed current technique to simulate corrosion of steel reinforcement in concrete," *Journal of Materials in Civil Engineering*, vol. 15, no. 1, pp. 41–47, 2003.

[18] S. A. Austin, R. Lyons, and M. J. Ing, "Electrochemical behavior of steel-reinforced concrete during accelerated corrosion testing," *Corrosion*, vol. 60, no. 2, pp. 203–212, 2004.

[19] R. E. Weyers, E. W. Weyers et al., *Concrete Bridge Protection and Rehabilitation: Chemical and Physical Techniques—Service Life Estimates*, Strategic Highway Research Program, National Research Council, Washington, DC, USA, 1994.

[20] American Concrete Institute Committee 222, *ACI 222R-01: Protection of MetaLs in Concrete Against Corrosion*, American Concrete Institute, 2001.

[21] Germann Instruments, 2006, RCT & RCTW, Summary of Germann Instruments, http:// www.germann.org/Brochures /RCT.pdf.

[22] H. Tabatabai, A. Ghorbanpoor, and M. D. Pritzl, "Evaluation of select methods of corrosion prevention, corrosion control, and repair in reinforced concrete bridges," Final Report, Wisconsin Highway Research Program, Madison, Wis, USA.